

Layered Structure of Room-Temperature Ionic Liquids in Microemulsions by Multinuclear NMR Spectroscopic Studies

R. Dario Falcone,^[b] Bharat Baruah,^[a, c] Ernestas Gaidamauskas,^[a, d] Christopher D. Rithner,^[a] N. Mariano Correa,^[b] Juana J. Silber,^[b] Debbie C. Crans,^{*[a]} and Nancy E. Levinger^{*[a]}

Abstract: Microemulsions form in mixtures of polar, nonpolar, and amphiphilic molecules. Typical microemulsions employ water as the polar phase. However, microemulsions can form with a polar phase other than water, which hold promise to diversify the range of properties, and hence utility, of microemulsions. Here microemulsions formed by using a room-temperature ionic liquid (RTIL) as the polar phase were created and characterized by using multinuclear NMR spectroscopy. ¹H, ¹¹B, and ¹⁹F NMR spectroscopy was applied to explore differences between microemulsions formed by

using 1-butyl-3-methylimidazolium tetrafluoroborate ([bmim][BF₄]) as the polar phase with a cationic surfactant, benzylhexadecyldimethylammonium chloride (BHDC), and a nonionic surfactant, Triton X-100 (TX-100). NMR spectroscopy showed distinct differences in the behavior of the RTIL as the charge of the surfactant head group varies in the different microemulsion environments. Minor changes in the

chemical shifts were observed for [bmim]⁺ and [BF₄]⁻ in the presence of TX-100 suggesting that the surfactant and the ionic liquid are separated in the microemulsion. The large changes in spectroscopic parameters observed are consistent with microstructure formation with layering of [bmim]⁺ and [BF₄]⁻ and migration of Cl⁻ within the BHDC microemulsions. Comparisons with NMR results for related ionic compounds in organic and aqueous environments as well as literature studies assisted the development of a simple organizational model for these microstructures.

Keywords: ionic liquid • micelles • multinuclear NMR spectroscopy • self-assembly

Introduction

Microheterogeneous environments, such as those found in reverse micelles (RM) and microemulsions have tremendous

promise for the nonstandard environments they present. Often, chemistries occur in these solutions that do not occur in homogeneous liquid solutions.^[1] The majority of studies on microemulsions solubilize water as the polar component, most frequently by using the standard anionic surfactant AOT (sodium di-ethylhexylsulfosuccinate). These studies juxtapose water properties such as polarity, viscosity, conductivity, and hydrogen bonding for bulk water and water confined to reverse micelles.^[2] Researchers have also prepared and studied waterless microemulsions where water has been replaced by polar solvents that possess relatively high dielectric constants and that are immiscible with the continuous nonpolar solvent.^[3] These nonaqueous reverse microemulsions have attracted interest from both a fundamental^[4] and a practical perspective.^[5] Nonaqueous microemulsions show similar stability regions of isotropic solutions to the analogous aqueous systems and they can be formed by using a variety of different surfactants.^[3a,j,6] As reaction media, these microemulsions are particularly attractive for water-sensitive reactants.^[7] Information on the organization of these systems will help to develop the future applications of these systems.

New waterless microemulsion systems employing room-temperature ionic liquids (RTILs) as the polar medium further expand the properties and potential use of microemulsions.^[8] A range of RTILs is known and generally includes one large hydrophobic ion combined with a counterion of

[a] Dr. B. Baruah, Dr. E. Gaidamauskas, Dr. C. D. Rithner, Prof. D. C. Crans, Prof. N. E. Levinger
Department of Chemistry
Colorado State University
Fort Collins, CO 80523-1872 (USA)
Fax: (+1)970-491-1801
E-mail: Debbie.Crans@Colostate.edu
Nancy.Levinger@Colostate.edu

[b] Dr. R. D. Falcone, Dr. N. M. Correa, Prof. J. J. Silber
Departamento de Química
Universidad Nacional de Río Cuarto
Agencia Postal # 3. C.P. 5800 Río Cuarto (Argentina)

[c] Dr. B. Baruah
Current address:
Kennesaw State University
Department of Chemistry & Biochemistry
1000 Chastain Rd., MB #1203, Kennesaw, GA 30144 (USA)

[d] Dr. E. Gaidamauskas
Current address:
Department of Bioelectrochemistry and Biospectroscopy
Institute of Biochemistry, Mokslininku str. 12
LT-08662, Vilnius (Lithuania)

[†] Research performed at Colorado State University.

Supporting information for this article is available on the WWW under <http://dx.doi.org/10.1002/chem.201002182>.

different size and shape.^[9] Negligible vapor pressure combined with excellent chemical and thermal stability, ease of recyclability, and widely tuneable properties, such as polarity, hydrophobicity, and solvent miscibility through appropriate modification of the cation and anion, makes the environmentally friendly RTILs a potential medium for a number of chemical processes. Plechkova and Seddon^[10] review a wide range of industrial processes that take advantage of the versatility of RTILs. For example, BASF has developed the BASIL (biphasic acid scavenging utilizing ionic liquids) process to produce generic photoinitiator precursor alkoxyphenylphosphines. Processing of complex molecules, such as cellulose and other complex polyfunctional molecules, which present challenges by using conventional solvents, are successfully carried out in RTIL.^[11] Such applications could expand to RTIL-microemulsion-type systems increasing processing versatility, whereas simultaneously reducing costs. The possibility of replacing water with RTILs to form structures similar to water-containing microemulsions has been demonstrated, and some properties of these complex systems have been characterized.^[8]

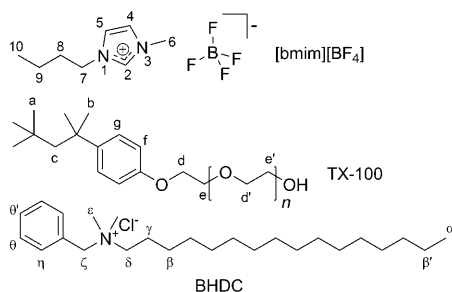
RTIL microemulsions have gained attention because of their potential as reaction and separation or extraction media.^[1,5] For example, a recent report has shown that surfactant-ionic-liquid-based microemulsions can be used to produce polymer nanoparticles, gels, and open-cell porous materials.^[8g] In the work presented here, we utilized 1-butyl-3-methylimidazolium tetrafluoroborate ([bmim][BF₄], Scheme 1) as the polar phase for microemulsions; this

using steady-state and picosecond time-resolved emission spectroscopy.^[8k] In addition, Gao et al. have shown that the interaction between the electronegative oxygen atoms of oxyethylene (OE) units of TX-100 and the electropositive imidazolium ring may drive [bmim][BF₄] to reside in the core of the TX-100/benzene aggregates.^[8c,e] The micropolarities of [bmim][BF₄]/TX-100/toluene were investigated with UV/Vis spectroscopy by using the absorption spectroscopy of methyl orange and methylene blue dye probes. The results indicated increasing polarity of the RTIL/oil microemulsion until a real RTIL pool formed, beyond which a relatively fixed polar microenvironment was obtained for the RTIL pool of the microemulsions. The properties of microemulsions are closely linked to the nature of the surfactant, especially the surfactant charges and the structures formed.^[13] Recently, Falcone et al. have reported formation of microemulsions by using the cationic surfactant, benzylhexadecyldimethylammonium chloride (BHDC, Scheme 1).^[8q] Cationic surfactants represent a surfactant subgroup, which forms microemulsions that enjoy many applications particularly in biology and industry.^[14] For the same ratio of polar solvent to surfactant, $w_s = [\text{RTIL}]/[\text{surfactant}]$ (commonly referred to as w_0 for water-containing reverse micelles) Falcone et al. noted particle formation larger than traditional reverse micelles solubilizing water.^[8q] Information on the structure and the organization of these systems would enhance their development and applications.

Here, we report studies employing multinuclear NMR spectroscopy to investigate the microemulsions containing RTIL, specifically, [bmim][BF₄], and demonstrate the dramatic difference in properties of these systems depending on the head group of the surfactant. Given the versatility of NMR spectroscopy and the presence of three NMR-active nuclei in the system (¹¹B,^[15] ¹⁹F,^[8b] and ¹H^[8b,c,e]) NMR spectroscopy is well suited for probing the structure and molecular organization in the RTIL microemulsions. The changes in chemical shifts provide direct information on the environment of both the cation and anion of the IL as well as the surfactant. The quadrupolar nature of the boron nucleus makes its signals particularly sensitive to its environment by using signal linewidths as probes in addition to chemical shift changes. These spectroscopic characterizations provide information on the layering of the component in these systems and the decreased viscosity of the ionic liquid in the interior of the reverse micelles.

Results

We have measured NMR spectra for three different NMR-active nuclei in each sample, ¹H, ¹¹B, and ¹⁹F. Because others have explored confinement of [bmim][BF₄] in TX-100/benzene microemulsions,^[8c,m,16] we used this system as a benchmark to provide comparison with the less-explored BHDC microemulsions. We also compared results for other microemulsions with the objective to provide a model for the molecular organization.



Scheme 1. Structures of [bmim][BF₄] (top), TX-100 (middle), and BHDC (bottom). Specific protons observed in NMR spectra are identified.

system is known to form organized structures in the presence of additives^[12] Researchers have demonstrated nano-sized reverse micelles dispersed with Triton X-100 (TX-100) in cyclohexane by using [bmim][BF₄].^[8a,c-e,k,m,p,q] Dynamic light scattering (DLS) confirmed that the RTIL microemulsions contained nanosized structures,^[8p,q] and similar to “classic” water-in-oil (w/o) microemulsions, the droplet volume of these nanosystems increase regularly as micelles were progressively swollen with added [bmim][BF₄].^[8m] In addition, several different studies have explored how confinement affects the RTIL. For example, solvation dynamics and rotational relaxation of coumarin 153 in [bmim][BF₄]/TX-100/cyclohexane microemulsions have been explored by

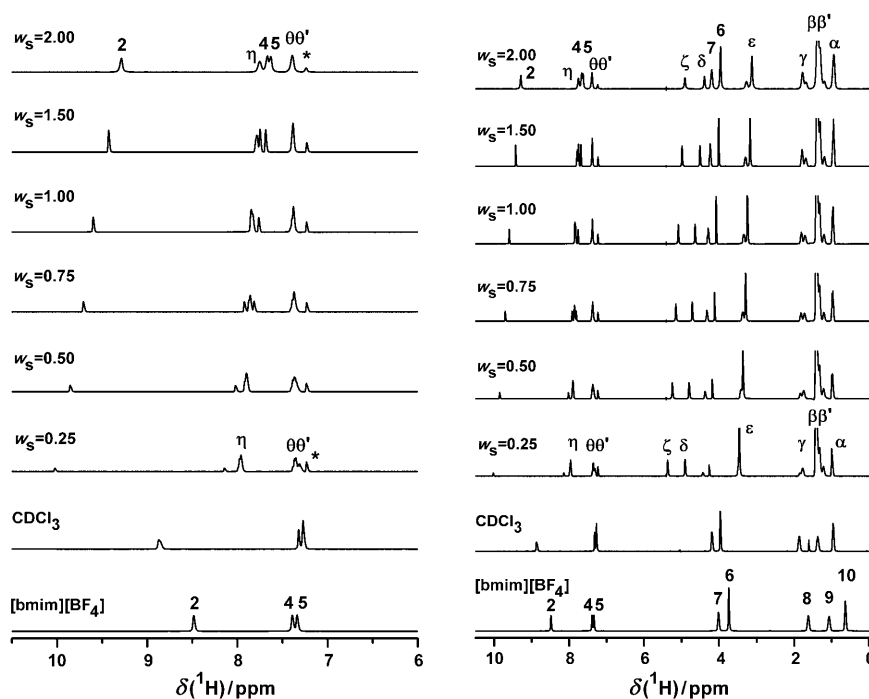


Figure 1. ^1H NMR spectra for neat $[\text{bmim}][\text{BF}_4]$, its solution in CDCl_3 , and BHDC/ $[\text{D}_6]$ benzene microemulsion samples. Labels refer to Scheme 1. Although samples were prepared with $[\text{D}_6]$ benzene, a small solvent signal is still evident, indicated by * (left: aromatic region, right: full-scale spectra).

^1H NMR spectroscopy: Figure 1 displays the ^1H NMR spectra collected for $[\text{bmim}][\text{BF}_4]$ in BHDC microemulsions. The ^1H NMR spectra of $[\text{bmim}][\text{BF}_4]$ in microemulsions reflect contributions from protons both on the $[\text{bmim}]^+$ ion and the surfactant as well as a negligible contribution from the nonpolar continuous solvent. We focused on the signal associated with the H2 of $[\text{bmim}]^+$ (see Scheme 1); the acidity of this hydrogen atom makes it particularly sensitive to its environment.^[17] As displayed in Figure 1, the H2 signal is significantly shifted downfield compared to the neat RTIL ($\delta = 8.48$ ppm). Even though this feature shifts upfield, toward the bulk value with increasing w_s , it remains substantially different from the bulk. This suggests a new environment for $[\text{bmim}][\text{BF}_4]$ in BHDC microemulsions.

The NMR spectra for $[\text{bmim}][\text{BF}_4]$ in TX-100 microemulsions, shown in Figure 2, differ from those for the RTIL in

BHDC systems. In contrast to the BHDC microemulsions, the $[\text{bmim}]^+ \text{H}_2$ signal shifts upfield smoothly toward its value in bulk $[\text{bmim}][\text{BF}_4]$ as the w_s value varies from 0.25 to 2.0. This shift suggests that the $[\text{bmim}]^+$ ion senses an environment approaching the bulk liquid as more RTIL is added to the system.

Signals for the surfactants, BHDC in Figure 1 and TX-100 in Figure 2 (see labels in Scheme 1), are also apparent in the spectra shown in Figures 1 and 2. Most of the signals associated with the BHDC protons display upfield shifts as w_s increases (Figure 1). In contrast, for proton signals associated with TX-100 (Figure 2) negligible shifts are observed. Overall, these results demonstrate that the ionic liquid affects the BHDC surfactant more than it

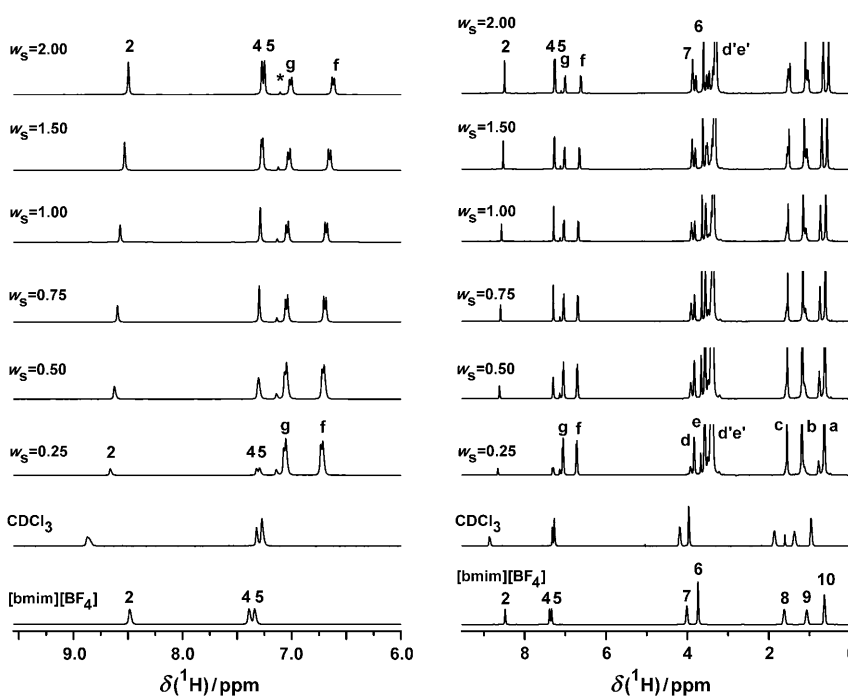


Figure 2. ^1H NMR spectra for neat $[\text{bmim}][\text{BF}_4]$, its solution in CDCl_3 , and TX-100/ $[\text{D}_6]$ benzene microemulsions. Labels refer to Scheme 1 (left: aromatic region, right: full-scale spectra).

does the TX-100 surfactant and suggest that the environment of the BHDC changes, whereas the environment of TX-100 remains relatively unchanged.

The various ^1H NMR signals in each spectrum allowed us to obtain specific structural details about the organization of the RTIL and the surfactant in the microemulsions. For example, in the BHDC-based microemulsions, the protons on the $[\text{bmim}]^+$ butyl group near H2 (H6 and H7) display larger shifts than H4 and H5, the two protons on the opposite side of the imidazolium ring (see Figure 1). This suggests directionality in the interaction sensed by H6 and H7; these protons experience a greater change than the other side of the ionic liquid cation. Corresponding shifts were not observed when the RTIL was added to TX-100 (see Figure 2). Likewise, we observed significant chemical shifts for the BHDC surfactant signals (see Scheme 1, Figure 1), arising from protons associated with the N-atom head group and the aromatic ring, much larger than in the long alkyl chain. These observations point to the interactions between surfactant and ionic liquid primarily involving the aromatic group and the N-atom head group on the surfactant and the H7, H2, and H6 side of the ionic liquid molecule. These observations contribute to the model we have developed for this system (see below). The large changes in shifts in both $[\text{bmim}]^+$ and BHDC stand in contrast to the spectra shown in Figure 2, for $[\text{bmim}]^+$ and TX-100, where very small or no shifts were observed. In the TX-100 system, the microemulsion environment leaves both surfactant and RTIL relatively unperturbed.

^{19}F NMR spectroscopy: Figure 3 shows representative ^{19}F NMR spectra for the neat RTIL and in the two microemulsion samples. The two signals arise in the NMR spectra due to the coupling of the ^{19}F nucleus with the two different boron isotopes, ^{10}B and ^{11}B , present in the $[\text{BF}_4]^-$ anion. The more intense signal corresponds to the more abundant isotope ^{11}B , which accounts for $\approx 80\%$ of the B atoms. Figure 4 displays the chemical shifts as a function of w_s for the two microemulsion samples. The chemical shifts from neat RTIL

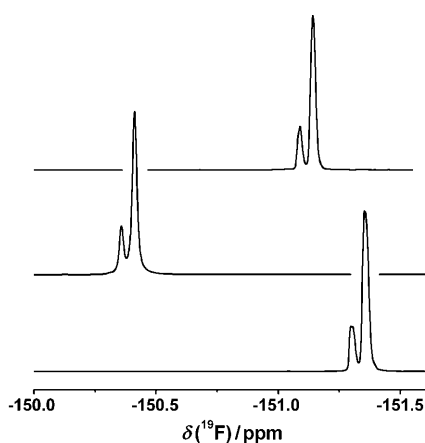


Figure 3. ^{19}F NMR spectra of $[\text{BF}_4]^-$ in neat $[\text{bmim}][\text{BF}_4]$ (bottom) and $[\text{bmim}][\text{BF}_4]$ in BHDC/ $[\text{D}_6]$ benzene ($w_s=2.0$, middle), and TX-100/ $[\text{D}_6]$ benzene ($w_s=2.0$, top) microemulsions. The two signals present in each spectrum reflect the influence of ^{10}B ($\approx 20\%$ abundant) and ^{11}B ($\approx 80\%$ abundant) isotopes.

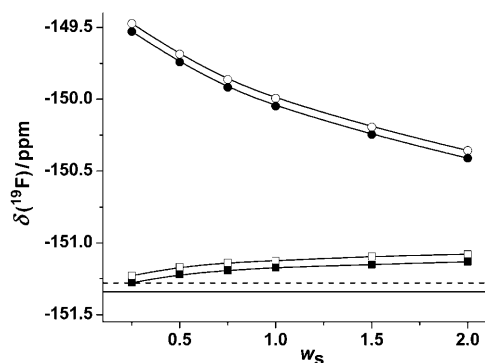


Figure 4. ^{19}F NMR chemical shifts of $[\text{BF}_4]^-$ in $[\text{bmim}][\text{BF}_4]$ microemulsions in BHDC/ $[\text{D}_6]$ benzene (circles) and TX-100/ $[\text{D}_6]$ benzene (squares) as a function of the amount of ionic liquid in the microemulsions. Open and solid symbols indicate the ^{10}B and ^{11}B signal positions, respectively. Horizontal lines indicate chemical shifts for $[\text{BF}_4]^-$ in neat $[\text{bmim}][\text{BF}_4]$; dashed and solid line indicate the ^{10}B and ^{11}B signal positions, respectively.

are shown as horizontal lines. From Figure 4, we note dramatic differences between the two different microemulsion samples. The fluorine signals from $[\text{BF}_4]^-$ in $[\text{D}_6]$ benzene/TX-100 reverse micelles display a minor shift downfield with increasing the ionic liquid content, diverging from the neat RTIL. In contrast, the fluorine signals in BHDC reverse micelles show a substantial shift upfield, toward the signals for the neat RTIL. However, the signals in BHDC never come close to the chemical shift in the neat RTIL or to the signals from fluorine in the TX-100 microemulsions.

In addition to changes in the ^{19}F NMR chemical shifts shown in Figure 4, we also noted variations in the ^{19}F NMR signal linewidths for the BHDC series of data, shown in Figure 5. Specifically, the linewidth decreases with decreasing w_s from 2 to 1, after which no further change is observed. For $w_s \geq 1$, the ^{19}F NMR spectra fit well to a single Lorentzian lineshape but signals from smaller w_s values require a Voigt profile (convolution of Lorentzian and Gaussian) to obtain an effective fit. These results suggest that some structural difference takes place near $w_s=1$. The combined chemical shift and linewidth data support the interpretation that the environment in reverse micelles prepared from BHDC and $[\text{bmim}][\text{BF}_4]$ differ substantially from the environment in reverse micelles prepared with nonionic surfactants.

^{11}B NMR spectroscopy: Figure 6 shows the chemical shift from the ^{11}B NMR signals of $[\text{BF}_4]^-$ in the two different microemulsion samples. For reference, the chemical shift observed in the neat RTIL is shown as a horizontal line. Boron signals in both systems display upfield shifts toward the value in neat RTIL. However, the signals from $[\text{BF}_4]^-$ in BHDC samples remain substantially shifted downfield compared with the neat RTIL, regardless of the w_s value, whereas the signals from $[\text{BF}_4]^-$ in TX-100 microemulsions appear to approach the value in the neat liquid.

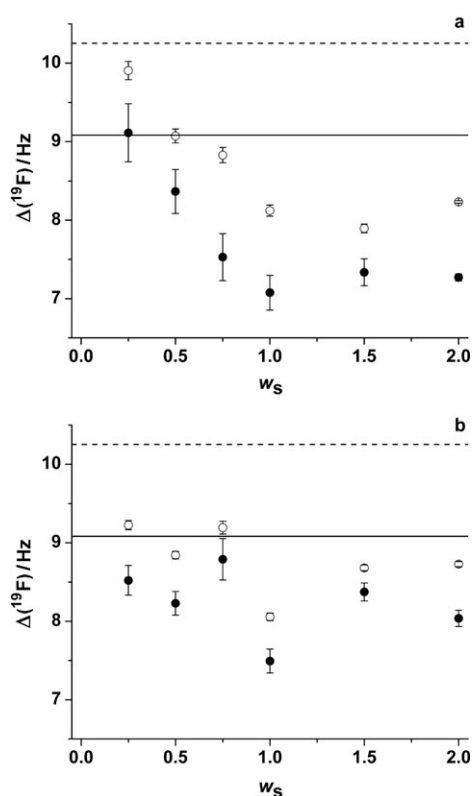


Figure 5. ^{19}F NMR signal linewidth as a function of w_s . Downfield (open symbols) and upfield (full symbols) resonance linewidths are shown for [bmim][BF₄]/BHDC/[D₆]benzene (a) and [bmim][BF₄]/TX100/[D₆]benzene (b) microemulsions. Open and solid symbols indicate the ^{10}B and ^{11}B linewidths, respectively. Horizontal lines indicate linewidths for [BF₄]⁻ in neat [bmim][BF₄]; dashed and solid line indicate the ^{10}B and ^{11}B signal positions, respectively. Two resonances were fitted into one Voigt function (Gaussian–Lorentzian amplitude cross product). Error bars show the 95% confidence intervals.

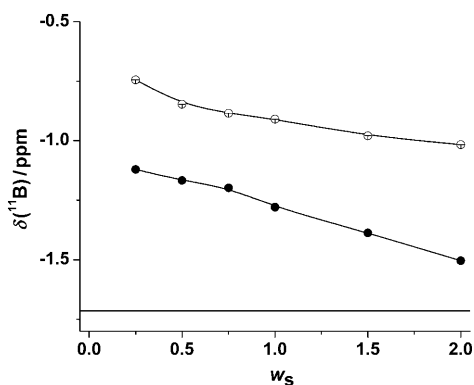


Figure 6. ^{11}B NMR chemical shifts of [BF₄]⁻ in [bmim][BF₄] microemulsions in BHDC/[D₆]benzene (○) and TX-100/[D₆]benzene (●) as a function of the amount of ionic liquid in the microemulsions. The horizontal line indicates the chemical shift for [BF₄]⁻ in neat [bmim][BF₄].

Linewidth data for the ^{11}B NMR spectra, shown in Figure 7, also provide insight into these microemulsions. In microemulsions formed by using BHDC, we observed insignificant changes in the ^{11}B linewidth, suggesting that the environment sensed by [BF₄]⁻ is similar to that in the bulk

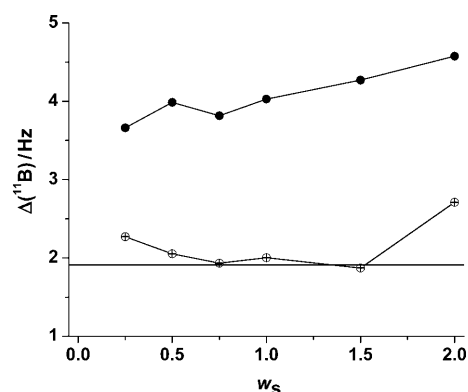


Figure 7. ^{11}B NMR resonance linewidth as a function of w_s in [bmim]-[BF₄]/BHDC/[D₆]benzene (○) and [bmim][BF₄]/TX100/[D₆]benzene (●). Forward linear prediction was used to extend the truncated fid decay from 0.1 to 0.5 s. Resonances were fitted as purely Lorentzian signals. Horizontal lines indicate linewidths for [BF₄]⁻ in neat [bmim][BF₄]. Error bars show the 95% confidence intervals.

liquid. However, for the ^{11}B NMR signal linewidth for microemulsions formed by using TX-100, the signal linewidth is half of that observed from the smallest w_s to the largest w_s investigated. In microemulsions including an aqueous phase, spectral linewidths have often shown increase, usually attributed to confinement or hindered molecular motion associated with the microemulsion environment, which is counter to the BHDC system.

Comparison systems—[bmim][BF₄] in organic solvents, model ionic compounds: To understand the nature of the RTIL components in the microemulsions, we have measured ^{11}B and ^{19}F NMR spectra of several model systems related to the RTIL-containing microemulsions. The model systems include dissolving [bmim][BF₄] in organic solvents, including methanol, acetone, acetonitrile, and chloroform. We have also added other ionic compounds, including Na[BF₄] and NaF, to the organic solvents to gauge the impact of the imidazolium ion on the [BF₄]⁻ spectrum. Chemical shift values for ^{11}B and ^{19}F from [BF₄]⁻ and F⁻ are given in Table 1. Trends in the ^{11}B NMR signal positions differ from those for ^{19}F . First, the ^{11}B chemical shifts in water, methanol, acetone, and acetonitrile systems appear insensitive to the nature of the cation, [bmim]⁺ or Na⁺. However, the ^{11}B chemical shifts for [BF₄]⁻ vary as a function of the organic solvent. In particular, the signals shift upfield for the more organic sol-

Table 1. ^{11}B and ^{19}F NMR chemical shifts [ppm] for model systems.

Solvent	Solute			
	[bmim][BF ₄] $\delta(^{11}\text{B})$	Na[BF ₄] $\delta(^{11}\text{B})$	[bmim][BF ₄] $\delta(^{19}\text{F}/^{10}\text{B}/^{11}\text{B})$	NaF $\delta(^{19}\text{F})$
water	-1.62	-1.59	-154.2/-154.2	-
methanol	-0.59	-0.62	-155.0/-153.4	-122.5
acetone	-0.33	-0.36	-151.5/-151.5	-
acetonitrile	-0.17	-0.21	-152.0/-152.0	-147.3
chloroform	-1.14	-	-152.6/-152.6	-
[bmim][BF ₄]	-1.86	-	-151.3/-151.3	-70.4/-70.4

vents when the polarity and/or the hydrogen-bond donor capacity of the solvent diminish. Interestingly, the chemical shift in the chloroform system is closer to the neat RTIL than it is in acetonitrile, acetone, or methanol. This suggests that the polarity of the added organic solvent is not the key in its impact on $[\text{BF}_4]^-$.

The ^{19}F NMR spectra continue to display two signals associated with the two different boron isotopes. At the same time, the ^{19}F chemical shift appears less sensitive to the changes in the polarity and/or the hydrogen-bond donor capacity of the solvent than the ^{11}B signals are. The signal corresponding to F^- (from NaF) appears in a region of the spectrum very different from that of the anion $[\text{BF}_4]^-$. Because we never observed a signal in a similar chemical shift region in the reverse micelles, we are confident that hydrolysis of the anion does not occur on the timescale of our experiments.

To simulate the interaction of the RTIL with the BHDC head group, we have added tetrabutylammonium chloride ($(\text{CH}_3)_4\text{NCl}$), into the neat ionic liquid and measured the ^1H , ^{11}B , and ^{19}F NMR spectra. The ^1H NMR spectra revealed a downfield shift for the $[\text{bmim}]^+$ H2 signal in the presence of $(\text{CH}_3)_4\text{NCl}$ ($\delta=8.55$ vs. 8.48 ppm recorded in neat $[\text{bmim}][\text{BF}_4]$). This follows the trend we observed for $[\text{bmim}][\text{BF}_4]$ in the reverse micelles. However, the impact of $(\text{CH}_3)_4\text{NCl}$ is substantially smaller than the intramicellar environment. The ^{11}B NMR signal shifts downfield to more positive delta values ($\delta=-1.23$ ppm) compared to the value in neat $[\text{bmim}][\text{BF}_4]$ ($\delta=-1.86$ ppm), similar to its behavior in reverse micelles. Finally, we observed a very small shift upfield for the fluorine signals with the addition of tetrabutylammonium chloride to the neat ionic liquid ($\delta=-151.01$ and -151.07 ppm). A similar effect is observed when NaF is dissolved in the pure RTIL ($\delta=-151.01$ and -151.07 ppm).

Combined, these chemical shift and linewidth observations for $[\text{bmim}][\text{BF}_4]$ with BHDC allowed us to propose a simple structural organization model shown in Scheme 2 and discussed further below.

Discussion

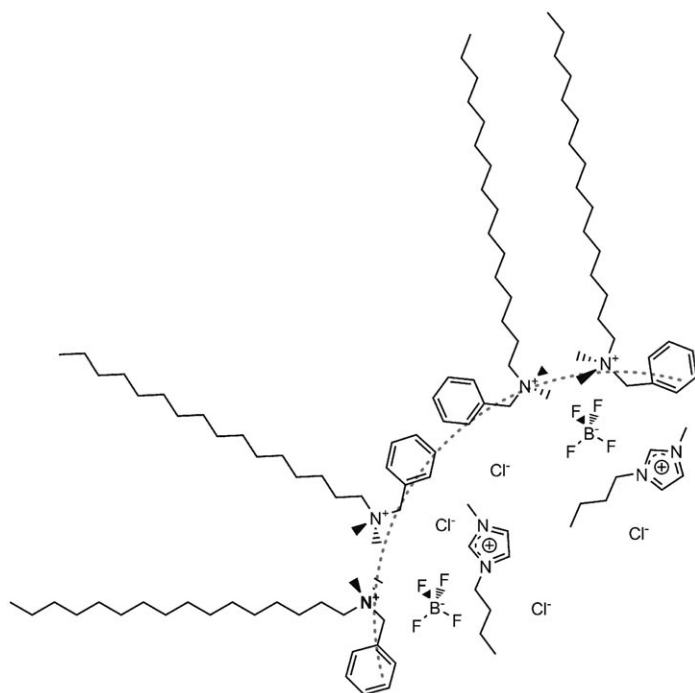
In traditional reverse micelles, those encapsulating water, the surfactant tends to form a well-defined boundary that delineates the water pool from the nonpolar solvent. Indeed, studies have invoked a core-shell model to describe the interior of the reverse micelles in which only a shell of water at the interface possesses properties that diverge from the bulk fluid.^[2d,18] In reverse micelles encapsulating solvents other than water, the microemulsion structure can diverge from well-defined shells in w/o microemulsions. For example, in reverse micelles encapsulating solvents such as ethylene glycol, several studies have shown that the polar solvent molecules penetrate the interfacial layer.^[7,19] Ionic liquids present a particularly interesting polar phase for microemulsions; these binary systems possess novel properties, which can lead to unique character in the microemulsions. With

the research presented we aim to obtain information about the structure of the RTIL in the microemulsion samples. To this end, we have performed studies by using both a nonionic and a positively charged surfactant.

To monitor each of the components in the RTIL microemulsions, we obtained NMR data from three different nuclei, which allows us to observe the effects of the microemulsion on the ionic liquid cation and anion, as well as allowing us to explore how the surfactants BHDC and TX-100 respond to encapsulation of $[\text{bmim}][\text{BF}_4]$. The use of nuclei with spin $1/2$ (^1H and ^{19}F), as well as spin $3/2$ (^{11}B) provided additional probing tools, namely linewidths and lineshapes that we have used to characterize this system. Results from previous NMR studies^[1d,20] and the mixed-solvent systems explored here (Table 1) together provide information for interpreting the NMR chemical shift data. Even though the ^1H NMR chemical shifts of the RTIL systems trend toward those observed in pure ionic liquid in the BHDC microemulsion samples, the signals remain different from the bulk values; this implies that a polar but different environment exists in the microemulsions. As shown in Figures 1 and 2, some signals from the RTIL shifted upfield and others shifted downfield. Such range in responses was previously reported for penetrating solutes in reverse micelles.^[13b,20] The chemical shifts of a range of model systems listed in Table 1 allowed us to gauge the polarity of the medium. Similarities between the ^{11}B NMR signals in organic solvents and in the BHDC microemulsions suggested that the environment around $[\text{BF}_4]^-$ may be less polar in $[\text{bmim}][\text{BF}_4]$ in BHDC microemulsions than it is in $[\text{bmim}][\text{BF}_4]$ in TX-100 microemulsions or the pure RTIL. However, the ^{19}F NMR signal shifted upfield for $[\text{BF}_4]^-$ in all solvent mixtures compared to the microemulsions and the pure RTIL. Both B and F atoms comprise the anion, so we interpreted these shifts not only to report on the location of the anion in a particular solvent, but on the electronic density within the anion. Increased polarity on the B atom is consistent both with the F atom increasingly pulling electron density from the B atom, and the B atom giving up this electron density. Increased electron density on the F atoms in the TX-100 systems also suggests that less electron density is given up by ion pairing in this system, as would be anticipated by comparing to the BHDC system with the positive surfactant surface. Combined, these results indicate that the RTIL interacts with the interfaces in both surfactant systems but that the interaction of $[\text{BF}_4]^-$ is more notable with BHDC than with TX-100.

The large shifts for the $[\text{bmim}]^+$ H2 signal observed in the ^1H NMR data shown in Figure 1 for the BHDC system suggests a dramatic change in the environment of $[\text{bmim}]^+$. The modest but observable chemical shift changes, also observed for the BHDC surfactant, demonstrate significant changes in structural organization. Even in bulk solution, some ionic liquids have shown the propensity to form regular 3D structures rather than remaining isotropic-like standard organic solvents.^[12] As a result, it is not surprising that the microemulsion environment could lead to RTIL organi-

zation.^[12] We observed large shifts in the ^{11}B and ^{19}F NMR spectra when $[\text{bmim}]^+$ interacts with $[\text{BF}_4]^-$ and these change when the surfactant supplants some of the interactions. Importantly, effects are observed in both the cation and the anion of the ionic liquid when combined with the surfactant suggesting a reorganization induced by the surfactant. One possible explanation for the dramatic change in the NMR spectra would be if the surfactant counter ion (Cl^-) exchanges with $[\text{BF}_4]^-$ as illustrated in Scheme 2. That



Scheme 2. Cartoon depiction of a possible organization for $[\text{bmim}][\text{BF}_4]$ in reverse micelles formed from BHDC in benzene.

is, in BHDC microemulsions $[\text{BF}_4]^-$ partitions to the interfacial region supplanting the regular Cl^- counterion and placing the $[\text{BF}_4]^-$ near the proximity of the positive-charged surfactant head group. ^1H NMR spectroscopy of $[\text{bmim}]\text{Cl}$ reveals a substantial shift downfield of H2 to $\delta \approx 10.5$ ppm, which is similar to chemical shifts observed in the ^1H NMR spectra of $[\text{bmim}][\text{BF}_4]$ in BHDC (Figure 1). Layering of RTILs has been observed in other systems, such as studies probing RTILs at surfaces.^[21]

We noted differences in the ^{11}B and ^{19}F NMR shift trends from the two different microemulsion environments. That is, for increasing w_s , chemical shifts for $[\text{BF}_4]^-$ in BHDC microemulsions always trend toward the value for the bulk RTIL. However, even in the largest system probed, $w_s = 2$, the chemical shifts remain drastically different from bulk. In TX-100 microemulsions, the ^{11}B NMR chemical shifts are closer to the bulk value and trend toward it with increasing w_s ; the ^{19}F NMR chemical shifts start almost at the value for bulk $[\text{bmim}][\text{BF}_4]$ and diverge slightly from that value as w_s increases. In contrast, linewidth data for ^{11}B NMR signals

show similar behavior for $[\text{BF}_4]^-$ in BHDC and in bulk RTIL, whereas the linewidths for $[\text{BF}_4]^-$ in TX-100 diverges dramatically (Figure 7). ^{19}F NMR linewidths are narrower for $[\text{BF}_4]^-$ in both microemulsion samples compared to bulk. We attributed chemical shifts and linewidth results for $[\text{BF}_4]^-$ in BHDC microemulsions to increased structure imposed on the RTIL. Interaction of the RTIL components with the cationic surfactant surface appears to provide a scaffold on which the RTIL can arrange. Although the TX-100 provides a surface, the nonionic nature of the surfactant leaves the RTIL relatively unstructured.

The data we have collected from NMR experiments suggests that in BHDC microemulsions, the RTIL exists in a layered structure, possibly in a structure like the one depicted in Scheme 2. The NMR data interpretation is consistent with $[\text{BF}_4]^-$ replacing chloride ions at the interface allowing $[\text{bmim}]^+$ to interact with the chloride ion in the layer removed from the interface. Falcone et al. have previously measured these microemulsions by using DLS and found that the solutions contain discrete particles, that is, reverse micelles.^[3f] By using this data, we estimated the number of RTIL and surfactant molecules in individual particles to provide further insight into the structure and properties of these systems. The $[\text{bmim}][\text{BF}_4]$ components take up enough room so that only a few molecules should reside at the interface, whereas other molecules form a core. From the DLS data,^[3f] as well as an approximation of the BHDC surface area given in the literature,^[22] we estimated the aggregation number, that is, the number of surfactant molecules comprising each particle. Values for some of the reverse micelles measured are given in Table 2. Although the sizes for these particles are quite large, the aggregation numbers are comparable to large water-containing reverse micelles.^[23] Interestingly, the number of $[\text{bmim}][\text{BF}_4]$ pairs we predicted to comprise each reverse micelle, last column in Table 2, is far lower than what we would predict from spherical droplets of $[\text{bmim}][\text{BF}_4]$ with the bulk density $\rho = 1.20 \text{ g cm}^{-3}$.^[24]

Table 2. Size^[a] and aggregation parameters for BHDC reverse micelles. Values were calculated assuming a spherical particle with the surface area of the BHDC molecule, $\sigma = 40 \text{ \AA}^2$ (from ref. [22]).

w_s	Particle diameter [nm] ^[a]	N_{agg}	# $[\text{bmim}][\text{BF}_4]$
1.0	11.5	1400	1400
1.5	25.8	5200	7800
2.0	49.4	19200	38400

[a] From reference [8q].

The ^{11}B NMR spectral linewidths we measured for $[\text{bmim}][\text{BF}_4]$ in the microemulsions showed different trends from chemical shifts. In particular, we observed largely the same linewidth for $[\text{BF}_4]^-$ in BHDC reverse micelles, whereas the linewidths for $[\text{BF}_4]^-$ in TX-100 reverse micelles were substantially broader. The linewidth of signals associated with quadrupolar nuclei generally increase compared to bulk solution when molecules are placed in standard water-containing reverse micelles.^[1d,25] Because NMR linewidths

depend on relaxation times and dynamical processes, increased linewidths for molecules in reverse micelles are generally interpreted as indicative of more viscous or restricted environments,^[25,26] or, alternatively, related to a dynamical processes such as chemical exchange of the probe under examination.^[25] The increased linewidth observed for TX-100 compared to bulk [bmim][BF₄] suggests that the nonionic reverse micelles present a more restrictive environment for [BF₄]⁻ than BHDC or the bulk RTIL. We might expect that the layering we propose for the BHDC system would lead to a more confining environment than bulk. However, the estimate for aggregation characteristics given above suggests reduced density for the [bmim][BF₄] in BHDC reverse micelles. These two effects, layering and density, could cancel each other leading to similar linewidths for both. The increasing linewidth for $w_s=2$ could indicate a regime where these effects no longer cancel each other.

So what can we glean from the data we have collected? Importantly, we noted dramatic differences between the systems formed by using BHDC, a surfactant with a cationic head group and anionic counterion, from those formed by using the nonionic TX-100 surfactant. In particular, BHDC seems to have a much stronger impact on a range of ionic liquid properties than TX-100 does. For example, at the lowest w_s values, the ¹H NMR signal from H2 of [bmim]⁺ appears almost 1.4 ppm further downfield in BHDC microemulsions compared to TX-100 microemulsions. In both systems, this signal shifts upfield toward the value for the pure RTIL. However, in BHDC microemulsions even at the highest w_s value, the H2 signal appears more than 0.6 ppm downfield from the value for the pure RTIL. We interpret these observations in terms of a simple structural model. The changes in chemical shifts are consistent with the exchange of Cl⁻ and [BF₄]⁻ anions resulting in a different type of layering in the RTIL/BHDC microemulsion. This demonstrates the different environment for [bmim]⁺ depending on the surfactant and promises well for the versatility of these systems.

Conclusion

The results presented in this work show that the nature of microemulsions sequestering room-temperature ionic liquids depends strongly on the nature of the surfactant used. The environment that induces the chemical shifts we observed for the BHDC microemulsions, includes significant structural differences compared to other RTIL microemulsions, mixtures of RTIL with organic solvents and other salts, as well as the pure RTIL. Indeed, none of the model systems came even close to providing the dramatic chemical shifts we observed in BHDC microemulsions. We have presented data that support the possibility that [bmim]⁺ and [BF₄]⁻ forms microstructures within the BHDC microemulsions causing layering to occur. That is, in BHDC microemulsions [BF₄]⁻ partitions to the interfacial region supplanting the regular Cl⁻ counterion. This puts [BF₄]⁻ in near proximity to the

ammonium surfactant head group and leaves [bmim]⁺ further away from the interface and interacting with the Cl⁻ counterions that migrated into the RTIL location.

Another important finding in this work is the minor changes observed for [bmim]⁺ in the TX-100 reverse micelles containing the ionic liquid, whereas the environment for [BF₄]⁻ shows significant differences. Considering that the cation is quite hydrophobic, one might have expected strong interactions between the cation and TX-100. These results have implications for researchers intending to use these environments for chemistry in confinement and encourage further explorations into these complex and potentially versatile systems.

Experimental Methods

Materials: Triton X-100 (TX-100, Sigma), and [D₆]benzene (Sigma, 99.9%) were used without prior purification. Benzylhexadecyldimethylammonium (BHDC, Sigma), was recrystallized in ethyl acetate.^[26] The surfactants TX-100 and BHDC were dried under vacuum before use. The room-temperature ionic liquid (RTIL) used, 1-butyl-3-methylimidazolium-[BF₄] ([bmim][BF₄], HPLC, ≥ 97.0% Sigma) was purified, by treatment with activated charcoal to remove colored impurities, filtering, and drying under vacuum at 60 °C for 4 h as described in the literature.^[27]

Tetramethylammonium chloride (N(CH₃)₄Cl, 99% Sigma), Na[BF₄], NaF, water, methanol, acetone, and acetonitrile were used without prior purification. All solvents were HPLC grade.

Microemulsion preparation: To prepare microemulsion samples, solutions of TX-100 or BHDC in [D₆]benzene were prepared by mass. In the TX-100/[D₆]benzene system, the surfactant concentration was 0.70 M, whereas in BHDC/[D₆]benzene, the surfactant concentration was 0.30 M. To these solutions, varying volumes of [bmim][BF₄] was added by using a microsyringe to yield $w_s=0-2$. The resulting solutions were clear solutions with a single phase. Above $w_s=2$, samples appeared cloudy indicating a phase change. The lowest value for w_s (0) corresponds to a system to which no [bmim][BF₄] was added.

Multinuclear NMR spectroscopic characterization of microemulsions: To compare the results obtained in BHDC microemulsions, we have measured ¹H, ¹¹B, and ¹⁹F NMR spectra of [bmim][BF₄] as a solute in various organic solvents. We have also measured the ¹¹B and ¹⁹F NMR spectra of Na[BF₄] and NaF solutes in the same organic solvents, to compare with the results obtained by using the RTIL. Thus, saturated solutions of [bmim][BF₄], Na[BF₄], and NaF in water, methanol, acetone, acetonitrile, and chloroform were prepared. To mimic the polar head of the cationic surfactant and the interaction with the RTIL, we measured NMR spectra of a saturated solution of N(CH₃)₄Cl in neat [bmim][BF₄].

NMR data for ¹H and ¹⁹F were collected by using a Varian INOVA-400 NMR spectrometer with a resonance frequency of 400.108 and 376.436 MHz, respectively. ¹¹B NMR data were collected by using a Varian INOVA-300 at 96.287 MHz. ¹H, ¹¹B, and ¹⁹F chemical shifts were referenced against a sample of tetramethylsilane, BF₃·diethyl ether complex (at 0.000 ppm) and CF₃C₆H₅ (at -63.900 ppm), respectively.^[89] ¹¹B NMR spectra were acquired with a 83.6 kHz spectral window, a 60° pulse angle, and a 0.096 s acquisition time with no relaxation delay for the INOVA-300. For the INOVA-400 spectrometer, spectra were acquired with a 39.2 kHz spectral window, a 60° pulse angle, and a 0.2 s acquisition time with no relaxation delay. For signal position measurements, a 15 Hz exponential line broadening was applied before Fourier transformation. All NMR data were processed by using MestReC 4.8.6^[28] and plotted and fitted by using OriginPro 7. All the experiments were carried out at (21 ± 0.5) °C. ¹H NMR spectra of neat [bmim][BF₄] and TX-100

appear in the Supporting Information as well as spectra of BHDC in benzene and CHCl₃.

Acknowledgements

This material is based upon work supported by the National Science Foundation under Grant No. 0628260. R.D.F. and N.M.C. also received support by grant CONICET-NSF from CONICET. J.J.S., N.M.C., and R.D.F. hold research positions at CONICET.

- [1] a) T. Dwars, E. Paetzold, G. Oehme, *Angew. Chem.* **2005**, *117*, 7338–7364; *Angew. Chem. Int. Ed.* **2005**, *44*, 7174–7199; b) H. Stamatidis, A. Xenakis, F. N. Kolisis, *Biotechnol. Adv.* **1999**, *17*, 293–318; c) K. Holmberg, *Adv. Colloid Interface Sci.* **1994**, *51*, 137–174; d) D. C. Crans, A. M. Trujillo, S. Bonetti, C. D. Rithner, B. Baruah, N. E. Levinger, *J. Org. Chem.* **2008**, *73*, 9633–9640.
- [2] a) M. S. Altamirano, C. D. Borsarelli, J. J. Cosa, C. M. Previtali, *J. Colloid Interface Sci.* **1998**, *205*, 390–396; b) M. Hasegawa, T. Sugimura, Y. Suzuki, A. Kitahara, *J. Phys. Chem.* **1994**, *98*, 2120–2124; c) N. M. Correa, M. A. Biasutti, J. J. Silber, *J. Colloid Interface Sci.* **1996**, *184*, 570–578; d) I. R. Piletic, D. E. Moilanen, D. B. Spry, N. E. Levinger, M. D. Fayer, *J. Phys. Chem. A* **2006**, *110*, 4985–4999.
- [3] a) A. Martino, E. W. Kaler, *J. Phys. Chem.* **1990**, *94*, 1627–1631; b) V. Arcoleo, F. Aliotta, M. Goffredi, G. LaManna, V. T. Liveri, *Mater. Sci. Eng. C* **1997**, *5*, 47–53; c) R. Aveyard, B. P. Binks, P. D. I. Fletcher, A. J. Kirk, P. Swansbury, *Langmuir* **1993**, *9*, 523–530; d) K. P. Das, A. Ceglie, B. Lindman, *J. Phys. Chem.* **1987**, *91*, 2938–2946; e) C. G. Elles, N. E. Levinger, *Chem. Phys. Lett.* **2000**, *317*, 624–630; f) R. D. Falcone, M. A. Biasutti, N. M. Correa, J. J. Silber, E. Lissi, E. Abuin, *Langmuir* **2004**, *20*, 5732–5737; g) R. D. Falcone, N. M. Correa, M. A. Biasutti, J. J. Silber, *Langmuir* **2000**, *16*, 3070–3076; h) M. Gautier, I. Rico, A. A. Z. Samii, A. Desavignac, A. Lattes, *J. Colloid Interface Sci.* **1986**, *112*, 484–487; i) A. Lattes, I. Rico, A. Desavignac, A. A. Samii, *Tetrahedron* **1987**, *43*, 1725–1735; j) A. Martino, E. W. Kaler, *Langmuir* **1995**, *11*, 779–784; k) C. Mathew, Z. Saidi, J. Peyrelasse, C. Boned, *Phys. Rev. A* **1991**, *43*, 873–882; l) I. Rico, A. Lattes, K. P. Das, B. Lindman, *J. Am. Chem. Soc.* **1989**, *111*, 7266–7267; m) R. E. Riter, J. R. Kimmel, E. P. Undiks, N. E. Levinger, *J. Phys. Chem. B* **1997**, *101*, 8292–8297; n) R. E. Riter, E. P. Undiks, J. R. Kimmel, N. E. Levinger, *J. Phys. Chem. B* **1998**, *102*, 7931–7938; o) A. A. Z. Samii, A. Desavignac, I. Rico, A. Lattes, *Tetrahedron* **1985**, *41*, 3683–3688; p) J. J. Silber, R. D. Falcone, N. M. Correa, M. A. Biasutti, E. Abuin, E. Lissi, P. Campodonico, *Langmuir* **2003**, *19*, 2067–2071; q) E. I. Tessy, A. K. Rakshit, *Bull. Chem. Soc. Jpn.* **1995**, *68*, 2137–2141.
- [4] S. Ray, S. P. Moulik, *Langmuir* **1994**, *10*, 2511–2515.
- [5] P. D. I. Fletcher, M. F. Galal, B. H. Robinson, *J. Chem. Soc. Faraday Trans. 1* **1985**, *81*, 2053–2065.
- [6] a) A. M. Durantini, R. D. Falcone, J. J. Silber, N. M. Correa, *ChemPhysChem* **2009**, *10*, 2034–2040; b) R. D. Falcone, J. J. Silber, N. M. Correa, *Phys. Chem. Chem. Phys.* **2009**, *11*, 11096–11100.
- [7] N. M. Correa, E. N. Durantini, J. J. Silber, *J. Phys. Org. Chem.* **2006**, *19*, 805–812.
- [8] a) H. X. Gao, J. C. Li, B. X. Han, W. N. Chen, J. L. Zhang, R. Zhang, D. D. Yan, *Phys. Chem. Chem. Phys.* **2004**, *6*, 2914–2916; b) Y. Gao, N. Li, L. Q. Zheng, X. T. Bai, L. Yu, X. Y. Zhao, J. Zhang, M. W. Zhao, Z. Li, *J. Phys. Chem. B* **2007**, *111*, 2506–2513; c) Y. Gao, J. Zhang, H. Y. Xu, X. Y. Zhao, L. Q. Zheng, X. W. Li, L. Yu, *ChemPhysChem* **2006**, *7*, 1554–1561; d) Y. N. Gao, S. B. Han, B. X. Han, G. Z. Li, D. Shen, Z. H. Li, J. M. Du, W. G. Hou, G. Y. Zhang, *Langmuir* **2005**, *21*, 5681–5684; e) Y. Gao, N. Li, L. Q. Zheng, X. Y. Zhao, J. Zhang, Q. Cao, M. W. Zhao, Z. Li, G. Y. Zhang, *Chem. Eur. J.* **2007**, *13*, 2661–2670; f) G. M. Sando, K. Dahl, J. C. Owrutsky, *Chem. Phys. Lett.* **2006**, *418*, 402–407; g) F. Yan, J. Texter, *Chem. Commun.* **2006**, 2696–2698; h) F. Gayet, C. El Kalamouni, P. Lavedan, J. D. Marty, A. Brulet, N. Lauth-de Viguerie, *Langmuir* **2009**, *25*, 9741–9750; i) Y. J. Zheng, W. J. Eli, G. Li, *Colloid Polym. Sci.* **2009**, *287*, 871–876; j) N. Li, Q. Cao, Y. A. Gao, J. Zhang, L. Q. Zheng, X. T. Bai, B. Dong, Z. Li, M. W. Zhao, L. Yu, *ChemPhysChem* **2007**, *8*, 2211–2217; k) D. Chakraborty, D. Seth, A. Chakraborty, N. Sarkar, *J. Phys. Chem. B* **2005**, *109*, 5753–5758; l) A. Chakraborty, D. Seth, D. Chakraborty, P. Setua, N. Sarkar, *J. Phys. Chem. A* **2005**, *109*, 11110–11116; m) J. Eastoe, S. Gold, S. E. Rogers, A. Paul, T. Welton, R. K. Heenan, I. Grillo, *J. Am. Chem. Soc.* **2005**, *127*, 7302–7303; n) J. H. Liu, S. Q. Cheng, J. L. Zhang, X. Y. Feng, X. G. Fu, B. X. Han, *Angew. Chem.* **2007**, *119*, 3377–3379; *Angew. Chem. Int. Ed.* **2007**, *46*, 3313–3315; o) Z. M. Qiu, J. Texter, *Curr. Opin. Colloid Interface Sci.* **2008**, *13*, 252–262; p) B. M. Su, S. G. Zhang, Z. C. Zhang, *J. Phys. Chem. B* **2004**, *108*, 19510–19517; q) R. D. Falcone, N. M. Correa, J. J. Silber, *Langmuir* **2009**, *25*, 10426–10429.
- [9] a) C. M. Gordon, *Appl. Catal. A* **2001**, *222*, 101–117; b) R. Sheldon, *Chem. Commun.* **2001**, 2399–2407; c) P. Wasserscheid, W. Keim, *Angew. Chem.* **2000**, *112*, 3926–3945; *Angew. Chem. Int. Ed.* **2000**, *39*, 3772–3789; d) T. Welton, *Coord. Chem. Rev.* **2004**, *248*, 2459–2477.
- [10] N. V. Plechkova, K. R. Seddon, *Chem. Soc. Rev.* **2008**, *37*, 123–150.
- [11] a) S. T. Handy, X. Zhang, *Org. Lett.* **2001**, *3*, 233–236; b) A. Pinkert, K. N. Marsh, S. Pang, M. P. Staiger, *Chem. Rev.* **2009**, *109*, 6712–6728.
- [12] S. Coleman, R. Byrne, S. Minkovska, D. Diamond, *J. Phys. Chem. B* **2009**, *113*, 15589–15596.
- [13] a) N. E. Levinger, L. A. Swafford, *Annu. Rev. Phys. Chem.* **2009**, *60*, 385–406; b) E. Gaidamauskas, D. P. Cleaver, P. B. Chatterjee, D. C. Crans, *Langmuir* **2011**, *26*, 13153–13161; c) P. L. Luisi, M. Giomini, M. P. Pileni, B. H. Robinson, *Biochim. Biophys. Acta* **1988**, *947*, 209–246; d) M. P. Pileni, *J. Phys. Chem.* **1993**, *97*, 6961–6973.
- [14] a) M. Zhang, Y. P. Wu, X. Z. Feng, X. W. He, L. X. Chen, Y. K. Zhang, *J. Mater. Chem.* **2010**, *20*, 5835–5842; b) S. S. Madaeni, E. Rostami, A. Rahimpour, *Int. J. Dairy Technol.* **2010**, *63*, 273–283.
- [15] a) A. Bagno, F. Rastrelli, G. Saielli, *Prog. Nucl. Magn. Reson. Spectrosc.* **2005**, *47*, 41–93; b) *Nuclear Magnetic Resonance and the Periodic Table* (Eds.: R. K. Harris, B. E. Mann), Academic Press, New York, **1978**, p. 459.
- [16] D. Seth, *J. Phys. Chem. B* **2007**, *111*, 4781–4787.
- [17] A. D. Headley, N. M. Jackson, *J. Phys. Org. Chem.* **2002**, *15*, 52–55.
- [18] a) A. M. Dokter, S. Woutersen, H. J. Bakker, *Proc. Natl. Acad. Sci. USA* **2006**, *103*, 15355–15358; b) A. M. Dokter, S. Woutersen, H. J. Bakker, *J. Chem. Phys.* **2007**, *126*, 124507; c) D. E. Moilanen, N. E. Levinger, D. B. Spry, M. D. Fayer, *J. Am. Chem. Soc.* **2007**, *129*, 14311–14318; d) D. Cringus, A. Bakulin, J. Lindner, P. Vohringer, M. S. Pshenichnikov, D. A. Wiersma, *J. Phys. Chem. B* **2007**, *111*, 14193–14207; e) D. Cringus, J. Lindner, M. T. W. Milder, M. S. Pshenichnikov, P. Vohringer, D. A. Wiersma, *Chem. Phys. Lett.* **2005**, *408*, 162–168; f) D. S. Venables, K. Huang, C. A. Schmuttenmaer, *J. Phys. Chem. B* **2001**, *105*, 9132–9138.
- [19] a) N. M. Correa, N. E. Levinger, *J. Phys. Chem. B* **2006**, *110*, 13050–13061; b) N. M. Correa, P. A. R. Pires, J. J. Silber, O. A. El Seoud, *J. Phys. Chem. B* **2005**, *109*, 21209–21219.
- [20] M. Vermathen, P. Stiles, S. J. Bachofer, U. Simonis, *Langmuir* **2002**, *18*, 1030–1042.
- [21] a) D. Wakeham, R. Hayes, G. G. Warr, R. Atkin, *J. Phys. Chem. B* **2009**, *113*, 5961–5966; b) S. Bovio, A. Podesta, C. Lenardi, P. Milani, *J. Phys. Chem. B* **2009**, *113*, 6600–6603; c) C. Kolbeck, T. Cremer, K. R. J. Lovelock, N. Paape, P. S. Schulz, P. Wasserscheid, F. Maier, H. P. Steinruck, *J. Phys. Chem. B* **2009**, *113*, 8682–8688; d) S. Perkin, T. Albrecht, J. Klein, *Phys. Chem. Chem. Phys.* **2010**, *12*, 1243–1247; e) M. Mezger, H. Schroder, H. Reichert, S. Schramm, J. S. Okasinski, S. Schoder, V. Honkimaki, M. Deutsch, B. M. Ocko, J. Ralston, M. Rohwerder, M. Stratmann, H. Dosch, *Science* **2008**, *322*, 424–428; f) M. Z. Bazant, M. S. Kilic, B. D. Storey, A. Ajdari, *Adv. Colloid Interface Sci.* **2009**, *152*, 48–88; g) H. C. Chang, J. C. Jiang, Y. C. Liou, C. H. Hung, T. Y. Lai, S. H. Lin, *J. Chem. Phys.* **2008**, *129*, 044506; h) T. Pott, P. Meleard, *Phys. Chem. Chem. Phys.* **2009**, *11*, 5469–5475; i) C. Chiappe, *Monatsh. Chem.* **2007**, *138*,

- 1035–1043; j) E. W. Castner, J. F. Wishart, H. Shirota, *Acc. Chem. Res.* **2007**, *40*, 1217–1227; k) S. Baldelli, *Acc. Chem. Res.* **2008**, *41*, 421–431.
- [22] D. Grand, A. Dokutchayev, *J. Phys. Chem. B* **1997**, *101*, 3181–3186.
- [23] A. Maitra, *J. Phys. Chem.* **1984**, *88*, 5122–5125.
- [24] Y. U. Paulechka, A. G. Kabo, A. V. Blokhin, G. J. Kabo, M. P. Shevelyova, *J. Chem. Eng. Ref. Data* **2011**, *55*, 2719–2724.
- [25] B. Baruah, D. C. Crans, N. E. Levinger, *Langmuir* **2007**, *23*, 6510–6518.
- [26] O. O. Okoturo, T. J. VanderNoot, *J. Electroanal. Chem.* **2004**, *568*, 167–181.
- [27] P. Nockemann, K. Binnemans, K. Driesen, *Chem. Phys. Lett.* **2005**, *415*, 131–136.
- [28] Mestrelab Research, S.L. Feliciano Barrera 9B–Bajo, 15706 Santiago de Compostela (Spain), <http://mestrelab.com/contact>.

Received: July 30, 2010

Revised: January 26, 2011

Published online: May 6, 2011